Ejection of dust by elastic waves in collisions between millimeter- and centimeter-sized dust aggregates at 16.5 to 37.5 m/s impact velocities

Gerhard Wurm,* Georgi Paraskov, and Oliver Krauss
Institute for Planetology, Wilhelm-Klemm-Strasse 10, D-48149 Münster, Germany
(Received 12 August 2004; revised manuscript received 13 December 2004; published 24 February 2005)

We report on experiments in which millimeter-sized SiO_2 dust aggregates consisting of (sub)-micrometer-sized grains impact into centimeter-sized targets that consist of the same kind of dust particles. The porosity of the granular targets is between 74% and 88%. Impact speeds are between 16.5 and 37.5 m/s with most impacts around 25 m/s. Compaction of the target by the impacting dust aggregate creates a crater which is several millimeters deep and 2–3 cm in diameter. We do not detect a significant amount of ejecta originating at the crater. We do observe a large amount of ejecta though. These are dust granules that are ejected from the whole target surface up to significant distances away from the impact site. This implies that elastic waves induced by the impact are an efficient mechanism to eject material. The estimated mass of these ejecta can be larger than 10 times the projectile mass. The ejecta velocity is uniform across the surface. It is typically 0.5% of the impact velocity. We apply these results to the problem of planetesimal formation. Under microgravity ablation of a dusty body or mass gain in a dust-dust collision might result. This depends on the parameters of the impact. Due to the low ejecta velocities, net growth is also possible in secondary collisions after an eroding primary collision if the body is placed in a gas flow. Thus, for a large number of typical conditions for dust-dust collisions in protoplanetary disks, formation of a larger body results from an impact.

DOI: 10.1103/PhysRevE.71.021304 PACS number(s): 96.10.+i, 43.40.+s, 47.15.−x, 96.35.−j

I. INTRODUCTION

A mechanical impulse incident on a granular medium can have several effects and applications depending on the properties of the impulse and the properties of the medium. Waves generated by an impulse at the surface can, e.g., be reflected by buried objects and by the granular medium itself and be measured afterwards on the surface [1]. This can be used to detect buried objects. Other kinds of impulse can significantly change the morphology of the granular medium. On the one hand, according to the Reynolds principle of dilatancy (slow) compression at a granular surface might lead to a decompaction of a larger part of the medium [2,3]. On the other hand, repeated impulse in the form of (weak) vibrations might lead to compaction [4]. All these impulses can be generated in different ways. One possibility often encountered in nature and used technically is the impact of an object into the granular medium. This might locally lead to a strong deformation up to creating a crater [5–7]. At high impact speed this will also eject material [5,8,9]. Such collisions are crucial for the understanding of many problems in planetary science. It is, e.g., believed that planet formation proceeds by a continuous sequence of impacts of smaller objects into larger dusty bodies, adding mass so that eventually planets might form. Usually the process is split up into several parts. In a first step kilometer-sized objects are formed by collisions. At this size of kilometers self-gravity becomes important for the further growth process and the bodies are usually called planetesimals. However, it is widely accepted that the process of formation of these planetesimals begins with individual dust particles colliding very gently with and sticking to each other [10,11]. Over the last decade a number of experiments have been carried out in the astrophysical community to verify this model [12–17]. They show that growth of centimeter-sized dust aggregates in general can be understood in terms of a binary collision model. During this first stage of growth aggregates of the same size collide at 1 mm/s or less. Once objects reach the size of several centimeters, the impact energy is sufficiently high to initialize the compaction of the aggregates. Then preferentially particle aggregates of different size collide at much higher velocities. A body of 1 m (still consisting of dust) might collide with smaller bodies at velocities of several tens of m/s [11,12]. The physics behind these collisions is placed somewhere between the physics of aggregates of dust grains and granular physics. Densely packed dust particles might act as larger individual granules as used in the experiments reported here. However, significant cohesive forces also exist between the dust granules. In addition, an impact can locally fragment the dust granules at the impact site. This is an efficient way of dissipating impact energy.

It is an open question if a mechanism exists by which these collisions of a larger body with a millimeter- or centimeter-sized object can lead to a net growth of the larger body in the absence of gravity as required by the standard model of planet formation. So far all experiments show that the larger body is usually losing mass (under microgravity). Therefore, just considering the impact itself might not be sufficient to explain growth of a larger body in the context of planet formation. However, a target eroded by an impacting projectile can reaccrete ejecta from a collision if the collision takes place in a gas flow. These secondary, slower collisions of fragments can add mass again and eventually lead to net growth [18–21]. The efficiency of this mechanism depends

*FAX: (+49) 251 8336301. Electronic address: gwurm@uni-muenster.de

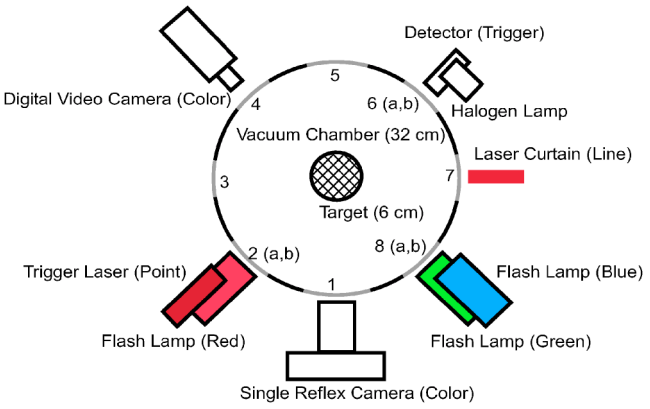

FIG. 1. (Color online) Sketch of the experiment setup. The impacts are carried out in a vacuum chamber at pressures below 10^{-2} mbar. A target tray is mounted in the middle of the chamber supported from below. Different light sources at different positions with different timing are used to illuminate an impacting projectile and rebounding particles. These are imaged by a digital photo camera and a video camera.

on the porosity of the body, the gas parameters, and the size and velocity of the ejected particles. The latter would typically need to be below 1 m/s or on the 1% level of the impact velocity considering the highest collision velocities to be 50–100 m/s. With this in mind we carried out experiments with millimeter-sized projectiles impacting centimeter-sized targets where both bodies are aggregates of submicrometer-sized dust particles. As explained in detail below especially the target is made of 0.5 mm granules of dust particles in most experiments. Thus, some of the observations made in our experiments might be explained by the physics of granular media with major modifications by aggregate physics on a smaller scale in some parts of the target.

Laboratory impact experiments are often carried out with the planetary scale of asteroids, planets, or moons in mind [6]. Then scaling laws, e.g., for crater sizes or ejecta mass are of importance. It should be noted that we do not carry out our experiments to scale them to any planetary size. The impact of a millimeter or centimeter dusty aggregate onto a somewhat larger dusty body at several tens of m/s is exactly what is supposed to happen in the early phase of planet formation. The only extrapolation which we will carry out is to estimate what the target response to the impact might be if it were slightly larger (50 cm). This is not a scaling in the way mentioned above. Our results are thus directly applicable to the process of planet (planetesimal) formation.

II. EXPERIMENTAL SETUP

A sketch of the experiment is shown in Fig. 1. The setup is part of a wind channel to allow studying the interaction between projectile, target, gas flow, and ejecta from a collision under conditions simulating protoplanetary disks. We only used the gas flow of the wind channel rudimentary so far for the experiments reported here. We will therefore only describe the impact part of the setup.

The impacts take place in a vacuum chamber (32 cm in diameter) that is evacuated prior to the impact to a pressure below 0.01 mbar. Gas drag at this pressure only slightly influences the trajectories for small submicrometer-sized particles. This is of minor importance here. Ejecta motion is otherwise determined by gravity. The target is an aluminum tray with 6 cm diameter and 5 cm depth filled with dust and centered in the middle of the chamber. Details of the target preparation will be given later. As projectile we use the same dust as in the target filled in a cylindrical (slightly conical) holder turned upside down. We currently use elastic support structures (aluminum foils) which only compensate the weight of the dust but easily bend during launch, allowing the projectile to pass. The projectile is launched by a compressed spring. To launch a projectile the holder is pulled upwards by a chain drive against the force of the spring. The projectile holder is connected to the chain drive by a rated break point. Once the spring is fully compressed, further pull will lead to a force exceeding the force tolerated by the contact and the contact breaks. The projectile holder (and the projectile within) is then accelerated by the spring and moves within a guide tube to approximately 15 cm above the target. The guide tube has two major functions. First it provides the necessary confinement for the spring and directs the projectile (holder) to the target. Second it has a stopper with a central hole at its end. The stopper abruptly decelerates the projectile holder. Due to inertia, the dust moves on through the central hole of the stopper. Thus a dust projectile is launched at the dust target. With the springs and holder currently used an initial maximum acceleration of approximately 7500 m/s^2 or 15000 m/s^2 is applied.

The interparticle forces holding the dust projectile together are relatively weak surface forces. Due to acceleration and friction of the dust with the walls of the holder, the dust projectile or parts of it can break up. However, the projectile mass for experiments where we analyzed images with respect to ejecta essentially remained confined to a volume comparable to the original projectile ($\sim$1 cm in size) if not noted otherwise [see, e.g., Figs. 2(a) and 2(b)].

In general an individual experiment might be described as follows: A target that has been under predefined low-humidity conditions for a few hours is weighed and placed into the vacuum chamber. The chamber is slowly evacuated to a pressure $p<0.01$ mbar. A projectile is then launched to the center of the target. By passing a light barrier a sequence of imaging is triggered.

As can be seen in Fig. 1 several (view) ports allow access to the chamber. Different positions of light sources have been used. One configuration described in the following section is shown in Fig. 1. Together with the trigger the green flash lamp is firing once. This results in an image of the incoming projectile in reflected light at a certain distance ($\sim$5 cm) above the target. At a time $t=0.5$ ms after the trigger the blue flash lamp is firing. This results in a second image of the incoming projectile. Due to the color separation, different information can be extracted from the color image of the camera. The camera's aperture is open during the whole experiment for a total time of 4 s. These first images reveal the overall size and shape of the incoming projectile. The projectiles look rather diffuse in reflected light. The video camera using the green flash as bright field illumination reveals an optically thick projectile though sometimes with a diffuse

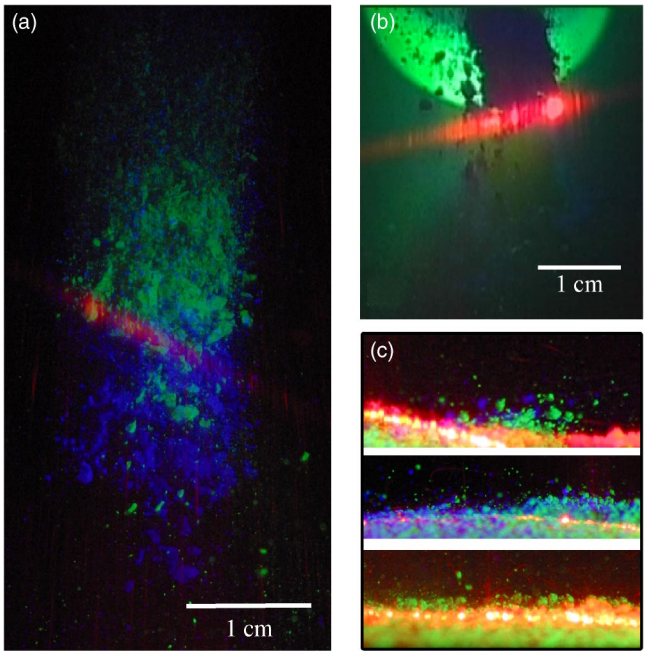

FIG. 2. (Color online) Impact imaging. (a) The projectile in reflected light. The green and blue flashes (upper and lower in black and white) are separated by 0.5 ms in time. Thus the distance between the two images of the projectile is a measure of the velocity. (b) The same projectile (~1 cm in size) viewed with the video camera in bright field illumination. As can be seen the projectile is optically thick. This seems to be in contrast to image (a). With respect to the projectile structure image (a) is deceiving. The ragged structure in image (a) is caused by rim particles casting shadows. (c) Images of ejecta leaving the target surface for three different experiments. For each image again two successive flashes in different colors have been used. Time difference between the flashes is 2.0 ms, approximately 15 ms after projectile impact, flash sequence is blue-green for the top and middle image, red-green for the bottom image. These images are shown for illustrative purpose here and give examples of cases where few fast particles are ejected (top), where gas flow is dragging particles along (middle) and where a whole layer of particles lifts off (bottom; also see Fig. 9). Different scales are used. The fragments are submillimeter in size.

rim. Probably a rim of small dust particles leads to self-shadowing in reflected light. The extent of the observed projectile in Fig. 2 roughly matches the size of the used dust projectiles. This was not the case for all experiments. In several experiments the projectile was spread out over a larger volume with a large number of smaller projectile parts. Due to the time difference between the flashes, the measured distance on the images gives the velocity of the projectile. This is, e.g., illustrated in Fig. 2.

In total a sequence of four flashes in two colors is used to illuminate the projectile and target which are imaged on the same frame. Projectile and rebounding fragments can well be separated. Thus a single color frame of the camera is used as high-speed photography. In addition a red laser sheet is used to image the trajectories of fragments in a fixed plane perpendicular to the target. After an impact the chamber is slowly filled with air and the target is removed. It is weighed again—i.e., after spending a few hours under the same low-

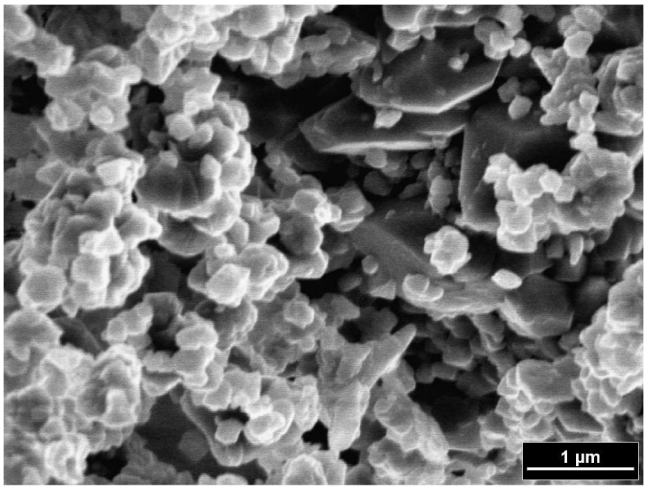

FIG. 3. Scanning electron microsocpe (SEM) image of the SiO_2 dust particles. This dust was used throughout all experiments.

humidity conditions as before. We are still continuously improving the setup. Thus not all experiments reported here have been carried out with the given configuration of light sources as indicated in Fig. 1.

III. RESULTS

Dust. As dust sample we used a commercial SiO_2 powder with a broad size distribution. Particle sizes are between 0.1 and 10 μm with 80% of the particle mass within particles of 1–5 μm in size. The particles have irregular shapes. The density of the bulk material is 2.6 g/cm^3. A scanning electron microscopy image of the dust is shown in Fig. 3. Earlier experiments show that the material itself is probably of minor importance for sticking of dust particles at least as similar materials like silicates are considered [12]. Thus we regard our dust as one possible analog material to model a large fraction of particles in protoplanetary disks or the solar nebula.

Target. We sieved the dust sample into the target tray to get a highly porous target. For most experiments we used a mesh with 0.5-mm openings for sieving. Dust mass added on top of a forming target in the sieving process is thus consisting of individual dust clumps which can be rather compact and are up to 0.5 mm in size, but loosely stick to other dust clumps. An image of a target can be seen in Fig. 4. The granular morphology of the surface due to the sieving is clearly visible. As porosity we define

$$P = \frac{V_{void}}{V_{total}}, \tag{1}$$

with V_{void} being the volume of the void space within the target not occupied by dust and V_{total} being the total volume of the target. The void space V_{void} is $V_{total} - V_{dust}$, with V_{dust} being the volume filled by solid material. With the dust mass measured and with the bulk density of the dust known (2.6 g/cm^3) V_{dust} can be determined and thus the porosity is given. Porosities varied between $P = 74\%$ and $P = 88\%$. Indi-

FIG. 4. A target prepared by sieving powder with a 0.5-mm mesh. The sieving results in a granular structure of the surface. The target diameter is 6 cm.

vidual errors are typically ±0.5% resulting from the determination of the average height of the target.

In some experiments the impact leads to a collapse of the target of a few millimeters over the whole width of the target. We attribute this to the vibrations (elastic waves) during the impact that are sufficient to compact the highly porous target slightly after the impact in combination with gravity. This effect can be separated though from the immediate response of the target to the impact which is visible on the surface on a much smaller time scale. As seen in Fig. 2(c) we can image the fragments leaving the target and distinguish them from the original surface. Furthermore, collapse of the target is restricted to targets that initially had a very high porosity approximately above $P=80\%$. This can be seen in Fig. 5 which also shows the tendency for more porous targets to collapse more strongly. The most porous targets were prepared by sieving through a 90-μm mesh. Thus the granules on the surface are smaller. Some of these targets started to collapse before the impact of the projectile. In these cases the launch vibrations which couple to the target via support structures were already sufficient to initiate the collapse. For most experiments we have observations showing that collapse does not start before the impact. We thus conclude that in these cases the effect of the impact dominates and is responsible for the outcome of the collisions as described below. This holds as far as crater formation or ejection of particles is concerned. However, the collapse shows that an impact has the ability to mobilize particles throughout the target.

It is certainly an interesting question what the effect might be if these experiments were carried out under microgravity. It is conceivable that the target might contract or expand. This has to be answered in future experiments.

For a series of targets we measured the change of porosity within the target. For these measurements we prepared the usual target and used a piston to push the dust upward in 5 -mm steps. We removed the dust above the target holder and measured the mass of the remaining target and so on. It might be assumed that the most porous layers are on top of the target. Indeed this is found as shown in Fig. 6. On average there is a slight decrease of porosity from the top layers to the bottom layers. Individual local porosities might significantly deviate from this mean curve though (marked as error bars). Whether this is important for the outcome of a

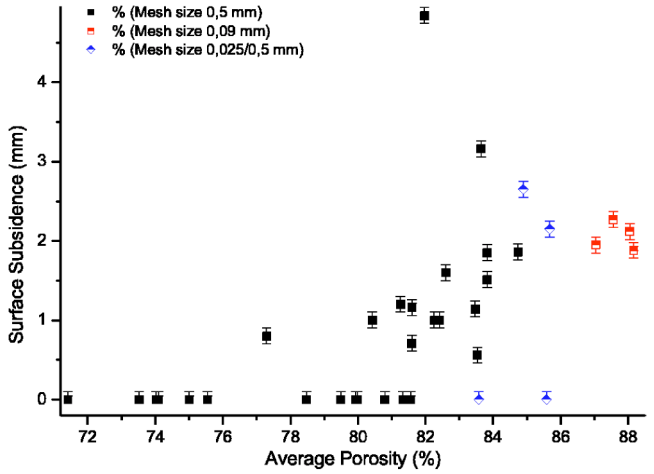

FIG. 5. (Color online) Subsidence of the target surface after an impact as a function of the average porosity of the target. The uncertainties in porosity are typically 0.5%. The bulk of the experiments were carried out with targets sieved through a 0.5-mm mesh. There is a tendency of increasing subsidence with increasing porosity. Approximately below 80% porosity the impact does not lead to a structural collapse within the target. The experiments with targets sieved through a 0.09-mm mesh resulted in higher average porosities and a rather well defined subsidence height. A few experiments have been carried out with a surface layer (~10 mm) of dust sieved through a 0.025-mm mesh onto a target otherwise prepared with a 0.5-mm mesh. With respect to subsidence these targets more or less behaved like targets only sieved with a 0.5-mm mesh.

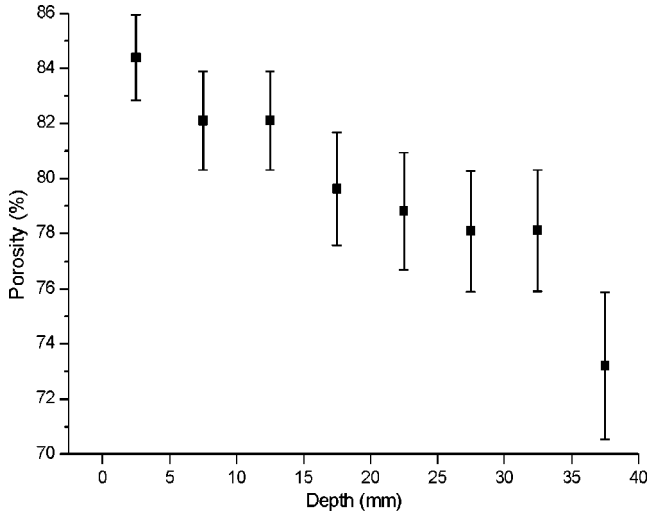

FIG. 6. Target porosity dependence on the vertical position in the target as typically used during the experiments. Marked as error bars is the standard deviation. The data are consistent with a linear dependence of porosity on the load (gravity of target material above a given position). If so, our target would be much more compressed by load than the targets prepared by Blum [22]. To avoid too much subsidence during an impact we slightly vibrated the target manually approximately after 2/3 of filling and before the top layer was filled in. The steps at 5 and 15 mm depth might thus be real and due to this process.

collision is not clear yet. If the decrease of porosity is due to the mass load by upper layers, then the effect is stronger for the targets we prepared compared to the dusty bodies generated by Blum [22] where no effect should be visible due to the small weight of the dust mass. However, we would like to avoid that due to gravity the surface of the target moves down too much during an impact as the vibrations lead to a compaction. In analogy to geology we will call this collapse in height subsidence. To avoid subsidence during impact we vibrated the target approximately after 2/3 of filling and before the top layer was filled in. The steps at 5 and 15 mm depth in Fig. 6 might thus be real and due to this process. In any case vibrations induce subsidence as well as the impacts do. This suggests that the effect of a collision might be more pronounced than a quasistatic compression because a larger part of the target particles are mobilized first.

The target is built up from granules that are typically 0.5 mm in size for most experiments and which themselves are rather compact consisting of (sub)micrometer-sized dust. These are two size scales which might be of importance. A most compacted layered body of contacting spheres of the same size would have a porosity of approximately $P=50\%$. Therefore, if the dust within the granules is densely packed and if the granules are also densely packed in the target, the overall porosity would be on the order of 75%. This is comparable to the porosities which we determine for the targets in our experiments. If during an impact mostly the larger granules as units are interacting, it might be of importance that they are packed rather densely even though the overall porosity looks high. One might easily think of targets with similar porosity but completely different morphology. Thus, impacts into targets of the same porosity could have different outcomes, e.g., with respect to ejecta and ejecta velocities.

Projectiles. For most experiments we used a slightly conical dust holder with an 8-mm-diam. opening on the bottom, 7 mm diameter at the top, and a length of 1 cm. In some experiments we filled the reservoir with dust compacted manually. We also inserted dust projectiles into the holder which were compacted outside the holder and inserted without force. An aluminum foil was used to prevent these projectiles from falling out while hanging upside down. The foil easily bends during launch. In these experiments most of the dust mass impacts as one projectile.

A. General description of the impacts

The impacts into highly porous targets resulted in craters of several millimeters in depth and 2–3 cm width. An example can be seen in Fig. 7. If the craters form by compaction due to projectile impact right on the spot of the impacting projectile, different projectile configurations (fragment distributions) should create quite different craters. This is essentially what we see. For one impact we had a stroboscopic imaging of a projectile which was fragmented to a large degree. If we take the light level on the image as a measure of the spatial distribution of the projectile fragments, they fit well with the crater profile in that experiment measured by scale paper slicing the crater. This suggests that the depth of the crater at a given position is proportional to the impacting mass. Within the small velocity range studied and the uncertain mass densities, we otherwise cannot give a correlation between impact speed and crater depth yet.

FIG. 7. Crater formed by an impact into the target (6 cm) at 25 m/s. This target's upper layer was sieved by a 25-μm mesh. Therefore, the surface looks less granular than the one in Fig. 4.

Sometimes the bottom of the crater qualitatively seems to consist of a number of slightly larger dust units compared to the original target. This might be larger fragments from the projectile but so far we have no way of distinguishing target particles from projectile particles. The fragmentation of the projectile certainly depends on the impact velocity. We note that we had two experiments where dust projectiles impact very slowly at about 2 m/s. In these two cases the original projectile could easily and unambiguously be reclaimed from the target afterwards since it remained in its original compact form of about 1 cm in size different from the granular material surrounding it which easily fell off after carefully lifting the projectile. It was buried in the target like an iceberg for 2/3 of its height.

B. Mass gain

One quantitative measure of the impact is the transfer of mass from the projectile to the target. We define mass gain as mass added to the target relative to the impacting projectile mass (not the target mass). Thus the overall mass of the target is not important here but only the fraction of mass it might lose or gain due to the impact. Figure 8 shows the mass gain as a function of the porosity of the target. This also includes data of very fragmented projectiles.

The mass gain shows no dependence on the impact velocity. A factor of 2 in impact speed does not show any influence on the amount of mass added to the target. This indicates that fragments are very slow and any variation in fragment speed is insignificant with respect to the escape velocity of the target (in our earthbound laboratory). This measure of mass gain is not to be confused with mass gain a target would have under microgravity conditions which would depend on the target size and the ejecta mass. Due to gravity, the ejecta in our experiments return to the target where they were ejected. Here the mass gain is to underline that most of the projectile is added to the target. Besides from any imaging these measurements allow one to determine an upper limit for the rebound velocities of fragments. Under vacuum a particle originating in the center of the target can reach the edge and is lost if it is faster than approxi-

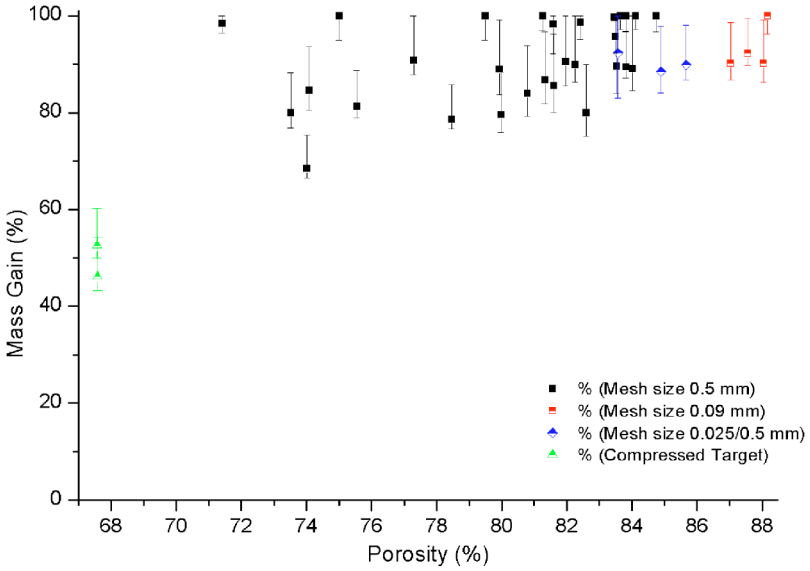

FIG. 8. (Color online) Net mass gain of the target with respect to the projectile mass as a function of the porosity of the target. The uncertainties in porosity are typically 0.5%. Mass gain is defined as mass added to the target relative to the impacting projectile mass (not the target mass). Thus the overall mass of the target is not important here but only the fraction of mass it might lose or gain due to the impact. The uncertainties in mass gain are mostly due to the uncertainties in determination of the projectile mass impacting the target. With each impact being individual the estimation of the uncertainties results in asymmetric error bars. The most porous targets were sieved with a different mesh size than the average target. Essentially the mass of the projectile is always added to the target. This shows that we do not miss any fast fragments that are too small to be imaged. Also shown are two experiments into compressed targets at the lowest porosity not described here which show a significant decrease in mass gain. This is in accordance to the imaging of a large number of fast fragments leaving these targets.

mately 0.5 m/s (assuming a rebound angle of 45°). This upper limit is only important for the smaller particles of up to several micrometers in size which cannot be imaged individually. For the larger particles the estimate of rebound speed is much better confined by the images as described in the next section. Thus, the mass gain here is to show that we do not miss any ejecta which are fast but too small to be imaged. However, in addition to the mass gain measurements we can also exclude a larger fraction of smaller particles since they would create a diffuse background on the images which we, e.g., see for impacts into compact targets but not here.

C. Fragments

We usually observed a certain amount of fragments rebounding from the target after a collision [e.g., Fig. 2(c)]. Particles that lift off approximately 0.1 mm from the surface can be detected. Due to gravity, the minimum detectable velocity is thus about 50 mm/s. If originating inside a crater or in the foreground or background of a dust pile velocities have to be higher for a particle to be imaged. E.g., at 5 mm crater depth the detection limit would be 0.3 m/s. We have two different measures of rebounding particles. The flashlamps give a snapshot at a predetermined time after impact. They are thus directly related to the impact. The laser sheet only shows particles passing a thin (<1 mm) layer perpendicular to the target surface.

We see no fragments which can unambiguously be traced back to the crater itself. In very few cases we observe a small amount of ejected fragments localized somewhere on the surface. We think that these might be the result of somewhat slower impacts of small individual projectile fragments [e.g., Fig. 2(c), upper image]. Estimates based on the images suggest that only a few percent of the total incoming projectile mass (if any) is within these rebounding fragments. Their velocities are between 0.4 and 0.8 m/s. Since they only account for a very small fraction of mass with respect to the projectile, we do not consider them to be of significance here.

A large amount of dust is ejected which is not correlated to the impact site but can be seen to emerge from the whole surface. These particles are all in a comparable height above the target even tracing the "skyline" of the target surface as can be seen in Fig. 9. Due to possible shadowing, the size of the imaged ejected granules does not always have to be the true size but a typical ejected particle has a size comparable to the sieve mesh size of 0.5 mm. In support of this, large parts of the target surface qualitatively look almost unchanged after an impact. The surface keeps its granular structure. Thus it is very likely that the size of the ejecta is identical to the size of the topmost layer of granules.

There is remarkably little scatter in the maximum height of ejected particles. While we cannot exclude slower or smaller fragments hidden, the sharp line of ejecta suggests rather steep upper cutoffs for rebound velocities for particles ejected in a direction opposite to the impact direction. No significant component perpendicular to the impact direction can be found.

The amount of ejecta is larger than the projectile mass. From the images it might be estimated that at least half of the

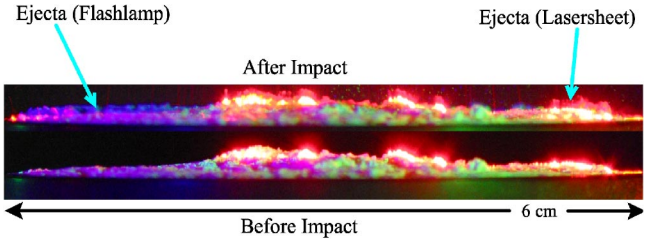

FIG. 9. (Color online) Target shortly after a collision with a projectile (top). As comparison an image of the target before the impact is shown below. The target has a 1 cm surface layer sieved by a 25-μm mesh on top of a target sieved by a 0.5-mm mesh. Ejecta can be seen in the blue flash on the left as well as in the laser curtain on the right. They show a constant maximum height for fragments all over the target surface.

surface lifts off. If all ejected dust units are 0.5-mm granules the ejected volume is about 10 cm^3. Thus about 10 times the mass of the projectile can be ejected. We are currently preparing experiments with larger targets but no data can be given yet. Since the low velocity of the ejecta is close to the limit detectable in a ground-based experiment, no further sampling of the mass could be done so far. Within our impact velocity range there is no significant dependence of the fragment speed on the impact velocity as seen in Fig. 10. While the impacts that were used to analyze the ejected particles are similar, projectile mass, size, and shape always vary slightly. Thus we cannot determine or exclude a dependence on impact energy or energy density (with respect to the projectile size) within our range of data. An important quantity for an impact is the coefficient of restitution, R, which we define here as

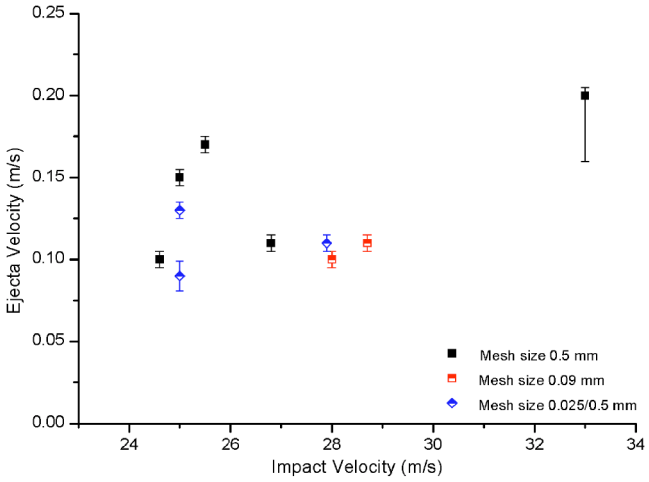

FIG. 10. (Color online) Velocities of particles ejected on the whole surface. Only experiments with a well-confined projectile and an unambiguous image of ejecta have been selected from the whole sample of experiments. An exception is the impact at 33 m/s where the main part of the projectile (which we assume to be well confined in this case) was not imaged which results in a timing uncertainty giving different error bars.

$$R = \frac{\nu_{eject}}{\nu_{imp}}, \tag{2}$$

with ν_{eject} being the speed of a particle ejected from the target after a collision and ν_{imp} is the impact velocity of the projectile. Within our impact velocity range the coefficient of restitution is $R=0.005\pm0.001$, which is very low.

The experiments imply that elastic waves are launched during the impact and that part of the top most layer of the target is lifted at the arrival of this wave. This requires sufficiently high momentum transfer as well as sufficiently low sticking of the top layer. The individual 0.5-mm dust units are only weakly bound by a small number of contacts via surface forces between dust particles. They easily roll down small slopes. Thus they can easily be ejected. In one experiment we vibrated the target slightly before the impact and the loose clumps rolled down to the base of a dust pile in the center to the outer target surface. During the impact essentially these particles lifted off. The particles that were bonded more strongly to their surrounding on the dust pile and that did not move due to the vibrations did not come off as numerous during the impact.

Since the lift height of the target surface does not significantly depend on the position on the surface, the waves seem to be well dispersed before reaching the surface. Thus this effect is probably not caused by waves traveling on straight lines from the crater to the surface since the strength should vary noticeable with distance. The momentum transfer responsible also has to be more or less opposite to the impact direction, since otherwise no preferred rebound direction of individual fragments at a given position on the surface can be found (Fig. 9). A wave reflected from the bottom of the target tray might be plausible though further studies are needed to confirm this. We measured the speed of sound in the targets to be between 45 and 50 m/s. Since our targets were about 50 mm in height we account for 2 ms between impact and fragment ejection at arrival of the wave in Fig. 10. Thus, we assume that a reflected wave is responsible for ejection.

Ejection itself might take up a significant part of the energy of the elastic wave. With 10 times the projectile mass at 0.5% of the impact velocity a fraction of 2.5×10^{-4} of the impact energy is distributed to the fragments. For an $m=0.3$ g projectile at approximately $\nu_{imp}=25$ m/s the impact energy is about $E_{imp}=0.1$ J. In addition some energy is used to break up the contacts. To estimate the amount of energy needed to break up contacts, we first estimate the number of contacts to support a granule. We will base our estimation of the number of contacts on geometrical arguments. As discussed above we assume that the ejected particles are the compact granules which we have sieved as last layer onto the surface of the target. We regard these 0.5 mm aggregates at the top essentially as individual solid spherical masses for simplicity here. However, each granule has a certain contact area with the granules below in which sticking of individual dust particles occurs. As radius of the contacting dust particles we take 1 μm. A compact granule thus has a "surface roughness" of about 1μm. On the one hand, if a granule were to have individual parts sticking out further from its

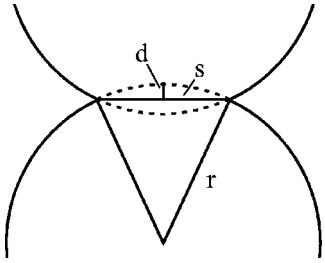

FIG. 11. Granule support model to estimate the number of contacts between dust particles at the intersection of two granules. If the rim thickness d is taken to be $d=1$ μm (dust particle radius) for an $r=250$ μm radius granule the radius of the cross section is $s=22.3$ μm. Thus the cross section is about 1600 μm^2. For 1-μm radius dust particles distributed in a chessboardlike manner on this area these are about 400 dust particles in contact.

surface before contact, these would easily be compressed first [12]. On the other hand, compression beyond the rim thickness is not possible for a compact granule. Therefore, in contact two granules will approximately intersect over the rim thickness of ~ 1 μm as indicated in Fig. 11. With this assumption the contact area between two spherical granules can be estimated to be about 1600 μm^2. For 1-μm (radius) dust particles this corresponds to $n=400$ particles in contact if we assume the particles to be arranged in a chess board like manner over the cross section. It has to be noted that this is only a rough estimate which will vary by a significant factor depending, e.g., on the size distribution of the used dust particles, granule size, or porosities.

The energy needed to separate two dust particles in contact is $E_{br}=10^{-15}$ J [12]. For 400 contacts energy on the order of 4×10^{-13} J is dissipated in breaking up the contacts of a single granule. Compared to the kinetic energy of 8×10^{-10} J of the granule after ejection this is a factor of 2000 less energy.

However, the wave will depend on the parameters of the impacting projectile and target (mass, velocity, size, porosity). Thus there might be a lower limit of the projectile size and impact velocity, e.g., of millimeter particles impacting at less than a few m/s, where the energy needed to break up the contacts would be larger than provided by the wave and no ejecta should be produced.

Only the experiments with a well-confined projectile are shown in Fig. 10. Images for dispersed projectiles can be interpreted less unanimously and are not shown but there is evidence that if a collective behavior of the surface can be detected at all, the motion is much slower, in agreement with the arguments given before. To determine if a significant part of fragments can be ejected at much lower impact energies, eventually microgravity experiments have to be carried out.

If a wave reflected on the bottom is responsible for ejection, then ejection at distances of 10 cm (2 times the height of the target) or more from the point of impact is possible. If no target tray were to support the dust, ejecta might be observed on the opposite side of the impact. This is supported by first tests of an impactlike impulse generated at the bottom of a dust target. If the target were much larger, e.g., meter sized, it is conceivable that no ejecta at all would be produced at the bottom side (opposite to the impact side). Already dilution of the energy density of a spherical wave would be a factor of 100 scaling from 10 cm to 1 m in size. Only a minor amount of damping would then lead to energy densities below the necessary threshold needed to break the contacts.

To study the effect of dust unit (granule) size which is determined by the sieving mesh we also prepared targets by sieving through a mesh of 90 and 25 μm. These targets consisted of much smaller dust units. The targets consisting of 90-μm dust units were the most porous targets we prepared with $P=88\%$. A few of them already collapsed due to the launch vibrations as mentioned before. Due to the time-consuming process of sieving, we filled the 25-μm targets on a base of 0.5-mm sieved targets with the top layer of 25-μm units being about 1 cm in height. Figure 9 actually is one of the 25-μm targets. As can be seen in Fig. 10 the ejecta velocities are comparable to the velocities of the larger dust units within the variations between individual experiments. Obviously there is little or no dependence of the ejection velocity on the granular size of the dust units if varied by a factor of 20. In general less massive (smaller) fragments will have fewer contacts. Under the same assumptions as given above a 25-μm granule would have $n=20$ contacts. The number of contacts is thus approximately increasing linearly with size. If the whole upper layer lifts off, the momentum transferred to the ejected particles at a given ejection velocity is also depending linear on the size of the granules. Thus, if the total momentum distributed to the next to upper layer is constant, so will be the ejection velocity, which is qualitatively in agreement with the observation.

IV. DISCUSSION

The amount of fragments from an impact of a $\sim$1-cm projectile into a highly porous dust target might be larger than 10 times the projectile mass. Eventually microgravity experiments are needed to detect all fragments and give a quantitative measure. Nevertheless, upper limits for velocities are already of importance to answer if planetesimal formation by growth can occur.

With respect to planetesimal formation it is often argued that impacts of millimeter- to centimeter-sized objects at several tens of m/s cannot lead to growth. Indeed our experiments show that an impact ejects more mass than the projectile adds. If no target tray were to support the bottom of the target (e.g., under microgravity) and ejecta were generated at the bottom, the target might in fact lose mass in the type of collision simulated in our experiments. We have to note though that impact velocities for a 10-cm body are most probably below 10 m/s in laminar protoplanetary disks and projectiles might on average be smaller [11]. As mentioned before for smaller projectiles, in a slower collision a plausible extrapolation of our data would imply that no ejecta at all might be visible.

Our impact velocities are more appropriate for a collision with the target being larger than about 50 cm in size. Scaling to this size dilution and damping of the elastic waves might also result in no ejecta at all. Thus immediate growth in a collision with a small dusty body is likely. This essentially

assumes that the elastic waves are spreading downwards from the impact site.

However, it is well known that a load applied to the surface of a granular medium spreads to the sides [3]. So it is conceivable that waves strong enough to eject particles might find a way back to the surface even in an unbound target. Also Hinch and Saint-Jean [23] found the interesting result that in the case of a solid particle impacting a line of other solid particles the impacting particle and many of the particles within the line can actually rebound. While their results can certainly not be directly applied here their calculations show though that quite unexpected effects might be seen in a discrete medium. Within this scheme it is also thinkable that local density variations maybe due to some previous compacting impact might scatter a wave upwards strong enough to eject particles.

If so, growth can still occur under conditions typical for protoplanetary gas-dust disks if we combine the experimental outcome of the impact with the effect of gas flow around and through these porous dusty bodies [20]. Wurm *et al.* [20] discuss how gas flow can return ejected particles if they are slow enough.

The idea is simply that gas motion directed toward the surface of the body can drag ejected particles back to the surface. For a solid body the streamlines of the gas will surround the body. However, through a porous dusty body a certain amount of gas will flow and the streamlines close to the surface of this body will enter it. If small ejected dust particles can couple to these streamlines, they will return to the surface. The fraction of ejecta mass that is reaccreted by this mechanism will depend on the porosity of the target, the gas parameters, and the ejecta parameters. Wurm *et al.* [20] assumed fragments to be micrometer-sized dust particles slower than 0.5 m/s. The speed of fragments ejected by elastic waves found in our experiments here is typically much below this threshold. Thus a small fragment could be reaccreted by gas flow.

We note that the collisions described here are subsonic. Since there might be collision velocities of 50 m/s and higher in protoplanetary disks, the transition region to weakly shocked impacts has to be studied in future experiments.

V. CONCLUSION

We carried out collision experiments between a porous dusty target of several centimeters in size with a granular morphology and dust projectiles with up to 1 cm in size at collision velocities between 16.5 and 37.5 m/s. While the impact of the projectile produces a crater no significant ejecta from the crater could be found. However, a large amount of material of 10 times the projectile mass is ejected over the whole surface of the target. These ejecta are very slow with velocities between 0.09 and 0.20 m/s in different experiments. Ejecta velocities are typically 0.5% of the impact velocity. Ejecta velocities for an individual impact are uniform over the whole surface, i.e., do not depend on the distance from the impact, and the particle motion is directed perpendicular to the target surface (bottom) with no detectable sideward motion. The ejecta velocity does not depend on the size of the granules (dust aggregates) building a target as varied from 0.5 to 0.025 mm. The experiments suggest different behavior for slower impacts of smaller projectiles, e.g., faster rebounding particles from the point of impact with no ejecta from other parts of the surface, but this has to be studied in more detail.

The ejection of particles from the whole surface can be explained by waves launched at impact and reflected at the bottom of the target tray. The launch of (elastic) waves might thus be an important mechanism to eject particles from a strongly cohesive, inelastic dusty medium. Depending on the size and morphology of the target net growth or ablation of a target under microgravity conditions results. Applied to the formation of planetesimals, growth or destruction of dusty bodies is possible, depending on the parameters of the impact.

ACKNOWLEDGMENT

This work is funded by the Deutsche Forschungsgemeinschaft.

[1] T. R. K. Mohan and S. Sen, Phys. Rev. E **67**, 060301 (2003).
[2] O. Reynolds, Philos. Mag. Ser. **50**, 469 (1885).
[3] J. Duran, *Sand, Powders, and Grains* (Springer, New York, 2000).
[4] J. J. Brey and A. Prados, Phys. Rev. E **68**, 051302 (2003).
[5] K. A. Newhall and D. J. Durian, Phys. Rev. E **68**, 060301 (2003).
[6] A. M. Walsh, K. E. Holloway, P. Habdas, and J. R. de Bruyn, Phys. Rev. Lett. **91**, 104301 (2003).
[7] H. J. Melosh, *Impact Cratering: A Geological Process* (Oxford University Press, Oxford, 1989).
[8] F. Rioual, A. Valance, and D. Bideau, Phys. Rev. E **62**, 2450 (2000).
[9] S. T. Thoroddsen and A. Q. Shen, Phys. Fluids **13**, 4 (2001).
[10] S. V. W. Beckwith, T. Henning, and Y. Nakagawa, in *Protostars and Planets IV*, edited by V. Mannings *et al.* (University of Arizona Press, Tucson, 2000), p. 533.
[11] S. J. Weidenschilling and J. N. Cuzzi, in *Protostars and Planets III*, edited by E. H. Levy and J. I. Lunine (*University of Arizona Press*, Tucson, 1993), p. 1031.
[12] J. Blum and G. Wurm, Icarus **143**, 138 (2000).
[13] J. Blum and M. Münch, Icarus **106**, 151 (1993).
[14] G. Wurm and J. Blum, Icarus **132**, 125 (1998).
[15] J. E. Colwell, Icarus **164**, 188 (2003).
[16] F. G. Bridges, K. D. Supulver, D. N. C. Lin, R. Knight, and M. Zafra, Icarus **123**, 422 (1996).
[17] T. Poppe, J. Blum, and T. Henning, Astrophys. J. **533**, 454 (2000).

[18] G. Wurm, J. Blum, and J. E. Colwell, Icarus **151**, 318 (2001).
[19] G. Wurm, J. Blum, and J. E. Colwell, Phys. Rev. E **64**, 046301 (2001).
[20] G. Wurm, G. Paraskov, and O. Krauß, Astrophys. J. **606**, 983 (2004).
[21] M. Sekiya and H. Takeda, Earth, Planets Space **55**, 263 (2003).
[22] J. Blum, in *Astrophysics of Dust*, edited by A. N. Witt, G. C. Clayton, and B. T. Draine, ASP Conference Series (ASP, San Francisco, 2004), Vol. CS-309, p. 369.
[23] E. J. Hinch and S. Saint-Jean, Proc. R. Soc. London, Ser. A **455**, 3201 (1999).